Biogeosciences

Geomorphic control on the δ^{15}N of mountain forests

R. G. Hilton[1], **A. Galy**[2], **A. J. West**[3], **N. Hovius**[2], **and G. G. Roberts**[4]

[1]Department of Geography, Durham University, Durham, DH1 3LE, UK
[2]Department of Earth Sciences, University of Cambridge, Cambridge, CB2 3EQ, UK
[3]Department of Earth Sciences, University of Southern California, Los Angeles, CA 90089, USA
[4]Bullard Laboratories, Department of Earth Sciences, University of Cambridge, Cambridge, CB3 0EZ, UK

Correspondence to: R. G. Hilton (r.g.hilton@durham.ac.uk)

Abstract. Mountain forests are subject to high rates of physical erosion which can export particulate nitrogen from ecosystems. However, the impact of geomorphic processes on nitrogen budgets remains poorly constrained. We have used the elemental and isotopic composition of soil and plant organic matter to investigate nitrogen cycling in the mountain forest of Taiwan, from 24 sites with distinct geomorphic (topographic slope) and climatic (precipitation, temperature) characteristics. The organic carbon to nitrogen ratio of soil organic matter decreased with soil ^{14}C age, providing constraint on average rates of nitrogen loss using a mass balance model. Model predictions suggest that present day estimates of nitrogen deposition exceed contemporary and historic nitrogen losses. We found ~ 6‰ variability in the stable isotopic composition (δ^{15}N) of soil and plants which was not related to soil ^{14}C age or climatic conditions. Instead, δ^{15}N was significantly, negatively correlated with topographic slope. Using the mass balance model, we demonstrate that the correlation can be explained by an increase in nitrogen loss by non-fractioning pathways on steeper slopes, where physical erosion most effectively removes particulate nitrogen. Published data from forests on steep slopes are consistent with the correlation. Based on our dataset and these observations, we hypothesise that variable physical erosion rates can significantly influence soil δ^{15}N, and suggest particulate nitrogen export is a major, yet underappreciated, loss term in the nitrogen budget of mountain forests.

1 Introduction

Nitrogen (N) is essential to primary productivity in the terrestrial biosphere (Evans, 1989; Vitousek and Howarth, 1991). The stock of bioavailable N influences an ecosystem's ability to buffer increases in atmospheric carbon dioxide through enhanced productivity (Oren et al., 2001), and also determines the impact of anthropogenic N deposition on plant growth and soil biogeochemistry (Aber et al., 1989; Matson et al., 1999; Zaehle et al., 2011). For these reasons, there have been considerable efforts to better understand the processes and rates of N loss from forests, and the factors which inhibit or amplify nutrient export (e.g. Hedin et al., 1995; Howarth et al., 1996; Lewis et al., 1999; Saunders et al., 2006; Schlesinger et al., 2006).

The loss of N from ecosystems can result in lateral fluxes of N compounds across the landscape. Rivers carry a signature of the dominant processes of N loss (gaseous, dissolved, particulate) and the rates at which they occur throughout catchments (e.g. Houlton et al., 2006; Brookshire et al., 2012a). River loads from undisturbed tropical forests reveal that particulate nitrogen (PN) export can be a significant loss term (Lewis et al., 1995). For example, the Madeira and Solimões rivers which drain the Andes to the Amazon River (McClain and Naimen, 2008) export ~ 0.2 t N km^{-2} yr^{-1} and ~ 0.4 t N km^{-2} yr^{-1} of PN, respectively. The PN flux is the largest single component of N exported from these catchments, and is approximately equal to the total dissolved N loss (Lewis et al., 1999). Even higher rates of PN export can occur from forests undergoing rapid physical erosion (Dadson et al., 2003; Milliman and Farnsworth, 2011), with mountain rivers exporting particulate organic carbon

(POC) derived from plant and soil organic matter at rates $> 10\,\mathrm{t\,C\,km^{-2}\,yr^{-1}}$ (Kao and Liu, 2000; Hilton et al., 2008a, 2012; Townsend-Small et al., 2008; Hatten et al., 2012). Despite its potential importance, the impact of physical erosion and PN loss on N cycling in ecosystems remains poorly constrained (Brenner et al., 2001; Amundson et al., 2003; Quinton et al., 2010). This is particularly the case for mountain forests, where PN transfers are not typically considered alongside dissolved N export (Saunders et al., 2006; McGroddy et al., 2008; Brookshire et al., 2012a; Huang et al., 2012), evolution of soil carbon stocks or POC transfer (Yoo et al., 2006; Hilton et al., 2008b, 2012).

Here we examine N cycling in the subtropical mountain forest of the Central Range, Taiwan, and assess the role of physical erosion as a driver of N loss in ecosystems. Erosion rates in this mountain belt are $3-6\,\mathrm{mm\,yr^{-1}}$ (Dadson et al., 2003), amongst the highest in the world (Milliman and Farnsworth, 2011). Topographic slope is the fundamental control on particulate export at the hillslope scale (Gilbert, 1909; Culling, 1960; Roering et al., 2001; Dietrich et al., 2003). Therefore, we have collected soil and plant organic matter from sites which randomly sample slope angle as an environmental variable and measured its N isotopic composition (reported as δ^{15}N, ‰), and organic carbon to nitrogen ratio (C/N), as well as the radiocarbon concentration of soil organic matter (reported as ^{14}C age, yr). The sites also span climatic conditions (temperature, precipitation), which are thought to play an important role for N cycling in ecosystems (Amundson et al., 2003). These samples provide a record of the integration of N inputs and outputs from the mountain forest over decades to millennia (Delwiche and Steyn, 1970; Mariotti et al., 1980; Handley and Raven, 1992; Högberg and Johannisson, 1993; Martinelli et al., 1999; Robinson, 2001), and in combination with a mass balance model (Shearer et al., 1974; Brenner et al., 2001) our measurements give new insight into the pathways of N loss and N cycling in mountain forests.

2 Study area and site characteristics

Taiwan is located at 22–25° N on the West Pacific margin at the convergence zone between the Eurasian and Philippine Sea plates. The Central Range mountains form the topographic spine of the island, $\sim 350\,\mathrm{km}$ long and $\sim 50\,\mathrm{km}$ wide with numerous peaks over 3000 m (Fig. S1). Mean annual precipitation (MAP) averages $\sim 2500\,\mathrm{mm}$ and can reach 6000 mm (Dadson et al., 2003). Much of this falls as rain during tropical cyclones that impact the island between June and October. The tectonic and climatic regime combine to produce high rates of physical erosion (Dadson et al., 2003) and build catchments where steep slopes are prevalent (Hilton et al., 2012). Vegetation grows up to the crests of the highest ridges and on the steep slopes, with the subtropical forest containing *Ficus*, *Machilus*, *Castanopsis*, *Quercus*, *Pinus*,

Tsuga, and *Picea* (Su, 1984). The above ground standing biomass stock in mixed conifer–hardwood forest of Taiwan is $\sim 22\,000\,\mathrm{t\,km^{-2}}$ (West et al., 2011), similar to the average estimated for the tropics (Dixon et al., 1994), making the mountain forest of Taiwan a suitable location to study the influence of climatic and geomorphic gradients on N cycling.

Samples were collected from sites on two east–west trending transects, separated north–south by $\sim 100\,\mathrm{km}$ (Fig. S1), on the mid- to upper-part of convex hillslopes. The northern transect was $\sim 30\,\mathrm{km}$ long and located mostly in the Liwu River catchment ($435\,\mathrm{km^2}$). The southern leg was $\sim 40\,\mathrm{km}$ long in the catchment of the Wulu River ($639\,\mathrm{km^2}$). Rates of POC export from these and other mountain catchments in Taiwan have been determined previously from direct sampling of rivers, returning yields of POC from vegetation and soil (Kao and Liu, 2000; Hilton et al., 2008a, 2012) after accounting for fossil POC input to the river sediments (Hilton et al., 2010). According to these estimates, the inter-annual rate of POC export from the Liwu and Wulu catchments was $6.8 \pm 2.7\,\mathrm{t\,C\,km^{-2}\,yr^{-1}}$ and $13.8 \pm 4.8\,\mathrm{t\,C\,km^{-2}\,yr^{-1}}$, respectively (Hilton et al., 2012). While some of this material may have derived from erosion of biomass by slope-clearing bedrock landslides (Hilton et al., 2011a; West et al., 2011), soil loss via overland flow is important for POC export from mountainous terrain (Larsen et al., 1999; Hilton et al., 2008a, 2012; Walker and Shiels, 2008; Hatten et al., 2012). Soil organic matter in Taiwan has an organic carbon to nitrogen ratio of ~ 12 (Kao and Liu, 2000). Hence, measured rates of POC export could correspond to a PN export of $\sim 1\,\mathrm{t\,N\,km^{-2}\,yr^{-1}}$ from the mountain forest. This estimate is consistent with other measurements from Taiwan in the Lanyang River catchment ($820\,\mathrm{km^2}$; Fig. S1), located in the north–east where erosion rates are lower (Dadson et al., 2003), where PN export from vegetation and soil is $0.4 \pm 0.2\,\mathrm{t\,N\,km^{-2}\,yr^{-1}}$ (Kao and Liu, 2000).

From 24 sites we collected 13 soil samples and 23 plant samples (Table S1). Samples were collected at discrete elevations (m), recorded using handheld GPS, to vary mean annual temperate (MAT). MAT was estimated using the sample site elevation and a saturated adiabatic lapse rate of $5\,^\circ\mathrm{C\,km^{-1}}$ combined with measured MAT (1981–2010) at sea level of 23.4 °C and 24.5 °C at Hualien (23.98° N, 121.60° E, northern transect) and Taitung (22.76° N, 121.15° E, southern transect), respectively (Fig. S1). The predicted MAT at Yushan (3950 m, 23.47° N, 120.26° E), 4.2 °C, is within 1 °C of the measured value (climate statistics for Taiwan, Central Weather Bureau, Taiwan http://www.cwb.gov.tw/eng/index.htm). To check that the isotopic composition of organic matter was representative of the sites, duplicate soil samples were collected at two sites, two plant species were sampled at four sites and six paired samples of soil and plant organic matter were collected.

Table 1. Correlation matrix (Pearson) for soil samples ($n = 13$) from the Central Range, Taiwan. Values in bold are different from 0 with a significance level of $\alpha = 0.05$; P values are given in parentheses.

Variables	MAT (°C)	MAP (mm)	Slope (sin θ)	C/N	^{14}C age (yr)
MAP (mm)	**−0.60**	–			
	(0.031)				
Slope (sin θ)	**0.63**	−0.11	–		
	(0.02)	(0.72)			
C/N	0.39	−0.22	0.11	–	
	(0.19)	(0.46)	(0.71)		
^{14}C age (yr)	−0.48	0.07	−0.45	**−0.83**	–
	(0.09)	(0.81)	(0.12)	**(0.0004)**	
δ^{15}N (‰)	**−0.70**	0.52	**−0.62**	−0.17	0.32
	(0.008)	(0.067)	**(0.025)**	(0.58)	(0.29)

In line with the objectives of this study, other attributes were not considered in site selection and are assumed to be sampled randomly. Decadal averaged MAP (mm) was obtained from a digital map gridded at 1×1 km (Dadson et al., 2003). Hillslope angle (θ, °) was determined using ArcInfo$^{\text{TM}}$ software, from a digital elevation model (40×40 m grid) and sampled over a 100 m length scale which is appropriate when considering erosion laws in mountain landscapes (Dietrich et al., 2003). Topographic slope was recorded as sin θ. The sample sites ranged between 530 m and 3190 m elevation, 7 °C to 21.9 °C MAT, 2060 mm to 3500 mm MAP, and had a slope angle θ between 7° and 50° (0.12 to 0.76 sin θ) (Table S1). We note that significant correlations exist between attributes of our soil sites (Table 1), with a negative relationship between MAT and MAP ($P = 0.03$) reflecting orographic forcing of precipitation, and a positive relationship between MAT and slope angle ($P = 0.02$). The latter is not observed for plant sample sites (Table 2).

3 Materials and methods

3.1 Samples

Plant samples were collected in March 2006 from *Pinus morrisonicola* (Taiwan white pine), selected for its ubiquitous presence across the full elevation range of forest (Su, 1984). Stems $\sim$ 5–10 mm in diameter (to provide an integration of several growing seasons) and less than $\sim$ 30 cm long were cut from live adult (> 4 m) specimens. In addition, stems of $\sim$ 1 m tall *Cymbopogon* sp. grasses were collected to investigate interspecies heterogeneity. Stems were stored in sterile sample bags and frozen less than one week after collection. After storage for one month, plant samples were oven dried at < 80 °C to remove remaining moisture. Bark was removed from pine stems and samples cut into $\sim$ 1 mg pieces and stored in sealed glass vials.

Table 2. Correlation matrix (Pearson) for *Pinus morrisonicola* and *Cymbopogon* sp. ($n = 23$) from the Central Range, Taiwan. Values in bold italic are different from 0 with a significance level of $\alpha = 0.05$; P values are given in parentheses.

Variables	MAT (°C)	MAP (mm)	Slope (sin θ)	C/N
MAP (mm)	**−0.70**	–		
	(0.0002)			
Slope (sin θ)	0.29	−0.07	–	
	(0.34)	(0.76)		
C/N	0.40	−0.32	0.23	–
	(0.06)	(0.14)	(0.29)	
δ^{15}N (‰)	−0.11	0.18	**−0.59**	−0.25
	(0.62)	(0.42)	**(0.003)**	(0.24)

Soil samples correspond to A–E soil horizons (variable humified organic matter intimately mixed with coarse and fine mineral fractions, bearing little structure of the original bedrock) were obtained at the same time as plants. Approximately 500 cm^3 of bulk material were collected over a depth of $\sim$ 10 cm and sealed in sterile bags, dried at 80 °C within one week of collection and decanted for dark storage within sealed sterile bags. To obtain an integrated bulk soil sample at each site, the entire sampled mass was then homogenised using a Cyclostec mill grinder. Inorganic carbon was removed from soils using a HCl leach (Hilton et al., 2010).

3.2 Measurement procedures and data analysis

Weight percent organic C (C$_{\text{org}}$, %) and N were determined on plant material and soil (following inorganic carbon removal) by combustion at 1020 °C in O$_2$ within a Costech elemental analyser (EA), normalised to an average of acetanilide standards and corrected for internal and procedural blanks as reported elsewhere (Hilton et al., 2010). Stable isotopes of organic C and N were analysed by a MAT-253 isotope ratio mass spectrometer coupled to the EA via Conflo-III and normalised based on measured values of standards (IAEA: N-1, NO$_3$) and laboratory standards

(oxalic acid and porano), corrected for internal and procedural blanks and reported in δ^{15}N and δ^{13}C notation relative to air (Mariotti, 1983) and Vienna Peedee Belemnite, respectively. For plant samples, to obtain desired amounts of N_2 for isotopic analysis large amounts of CO_2 were produced. A CARBOSORB^{TM} trap was used to scrub CO_2 prior to its introduction to the EA GC-column. For soils, ^{14}C concentrations were determined, after graphitisation of CO_2, by accelerator mass spectrometry at the UK National Environmental Research Council Radiocarbon Facility and are reported as ^{14}C age.

Precision (2σ) and accuracy of stable isotope measurements were determined using IAEA 600 and USGS-40 standards. Measured mean δ^{15}N were 1.2 ± 0.2‰ (IAEA 600, $\pm 2\sigma$, $n = 28$) and -4.5 ± 0.5‰ (IAEA USGS-40, $\pm 2\sigma$, $n = 18$), and mean δ^{13}C -27.6 ± 0.3‰ (IAEA 600, $\pm 2\sigma$, $n = 30$), indicating average accuracies of 0.1‰ and -0.1‰ for δ^{15}N and δ^{13}C, respectively. Further replicates of soil samples returned average 2σ of ± 0.4‰ ($n = 8$) and ± 0.3‰ ($n = 19$), for δ^{15}N and δ^{13}C, respectively. Average precision on ^{14}C age measurements was 72 yr (2σ). The inorganic removal procedure did not alter the measured δ^{15}N of the soil materials beyond this precision according to a comparison with aliquots not subjected to the acid leach, which conforms with results from soil materials elsewhere (Brodie et al., 2011), nor did it alter the ^{14}C age and δ^{13}C of treated IAEA standards (Hilton et al., 2008a). The measured variables were analysed for statistically significant inter-correlation using OriginPro^{TM}. Mean values of sample sets are reported $\pm$ the standard error of the mean throughout.

4 Results

4.1 Dataset size

The number of sample sites was relatively few across the two transects studied in Taiwan. In a global completion, Amundson et al. (2003) have previously assessed the role of dataset size for the return of significant correlations between plant and bulk soil δ^{15}N values and environmental variables. They showed that the statistical link between δ^{15}N and site conditions (in their case MAP and/or MAT) were preserved both when the number of sites were similar to this study ($n < 30$) and with ~ 4 times the number of sites studied in Taiwan. These findings are consistent with the results of Körner et al. (1988), who report significant correlations between the isotopic composition of plants and site elevation which are preserved in sample sub-sets with $n < 30$. We are therefore confident that the number of sites in this study can inform us of the first-order environmental controls on the measured δ^{15}N of Taiwan plants and soil.
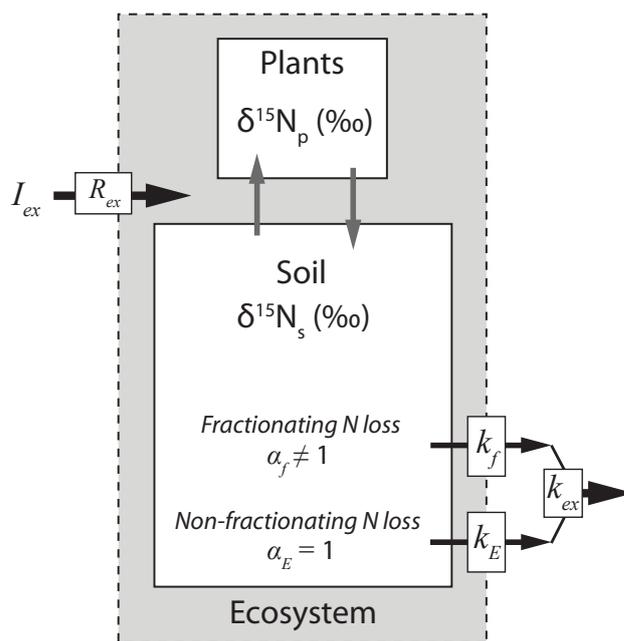

Fig. 1. Controls on the bulk δ^{15}N of a forest ecosystem with external N input and output (black arrows) and internal N cycling (grey arrows). The isotopic ratio of external inputs (R_{ex}) delivered at a rate I_{ex} (t N km^{-2} yr^{-1}) are modified by N losses which fractionate N isotopes by a factor α_f ($\neq 1$) by the rate constant k_f (yr^{-1}). N can also be lost by non-fractioning pathways ($\alpha_E = 1$) which occur at a rate k_E (yr^{-1}). The total N loss rate constant, $k_{ex} = k_f + k_E$.

4.2 Vegetation

Stems of *P. morrisonicola* had an average δ^{15}N $= -0.4 \pm 0.7$‰ ($n = 14$) and exhibited a ~ 6‰ range from -2.4‰ to 3.7‰ (Fig. 2; Table S2). The grass samples collected at the same site ($n = 4$) had a small (1.0‰), non-systematic average difference in δ^{15}N from *P. morrisonicola*, which was small when compared to the range of measured values. For *P. morrisonicola*, δ^{15}N was significantly ($P = 0.006$) negatively correlated with slope (Fig. 3), with no statistical link between δ^{15}N and MAP or MAT. When the two species were combined ($n = 23$), the mean δ^{15}N $= -0.9 \pm 0.5$‰ and the negative correlation between δ^{15}N and slope angle was strengthened ($P = 0.003$), remaining the only statistical link to a site attribute (Table 2).

P. morrisonicola stems had an average δ^{13}C $= -28.1 \pm 0.3$‰ ($n = 14$), and δ^{13}C values were positively correlated with elevation ($P = 0.003$) in agreement with trends observed in C3 plants elsewhere (Körner et al., 1988). This suggests that the sampled organic matter was in equilibrium with environmental conditions at the sites. *Cymbopogon* sp. had higher δ^{13}C values (Table S2), indicative of a C4 plant (Smith and Epstein, 1971).

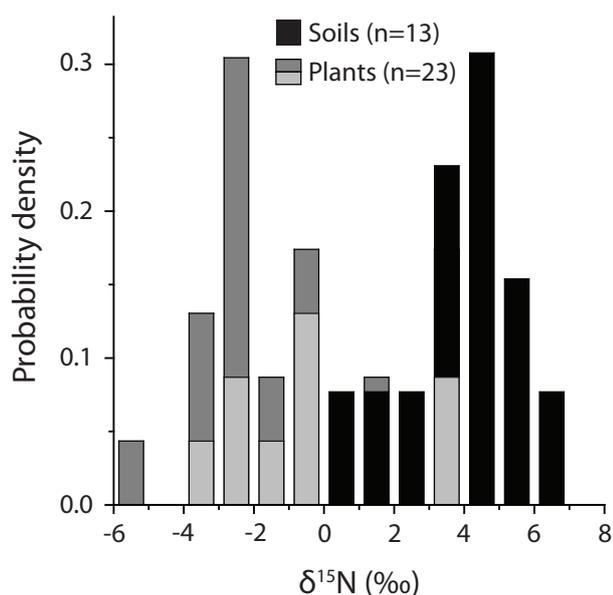**Fig. 2.** δ^{15}N of soil and plant organic matter from the Central Range, Taiwan. Probability density shown for soil (black), *Pinus morrisonicola* (dark grey) and *Cymbopogon* sp. (light grey).

4.3 Soil

The bulk C/N ratios of soil organic matter ranged between 3 and 14 (Table S3) and were similar to those reported elsewhere in Taiwan (Kao and Liu, 2000). A significant negative correlation ($P = 0.0004$) existed between C/N and ^{14}C age of bulk soil across all sample sites (Table 1). This correlation is not compatible with mixing of fossil organic matter from sedimentary bedrock (infinite ^{14}C age, C/N $\sim$ 5–10) with vegetation (Hilton et al., 2010). Instead, the ^{14}C depletion represents aging of organic matter. Soil ^{14}C age was not correlated with the climatic and geomorphic characteristics of the sample sites, or with δ^{15}N values (Table 1).

The average δ^{15}N of bulk soil was 4.0 ± 0.5‰ ($n = 13$) and ranged over $\sim$ 6‰ from 0.7‰ to 6.5‰ (Fig. 2). These values are similar to published measurements from soils in other locations in Taiwan (Kao and Liu, 2000; Liu et al., 2006). δ^{15}N values of duplicate and triplicate samples collected at two of the sites (Tables S1 and S3) were indistinguishable within the analytical uncertainty of 0.4‰, with means of 6.2 ± 0.3‰ ($n = 2$) and 4.5 ± 0.3 ($n = 3$), indicating that measured soil δ^{15}N values can be taken as representative site averages.

Soil δ^{15}N values were significantly, negatively correlated with slope ($P = 0.025$; Table 1) and displayed a similar relationship as plant δ^{15}N (Fig. 3). A negative relationship existed between δ^{15}N and MAT ($P = 0.008$) and δ^{15}N was positively correlated with MAP, but not significantly at the 95 % level ($P = 0.07$). Correlations amongst δ^{15}N and MAT and MAP were not observed in the larger vegetation sample set

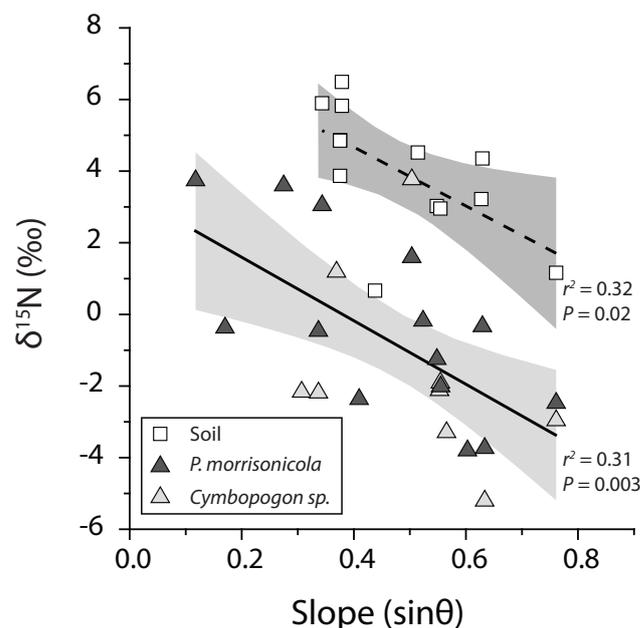**Fig. 3.** Relationship between topographic slope ($\sin \theta$) and δ^{15}N of soil (squares) and plants (triangles, *P. morrisonicola* in dark grey and *Cymbopogon* sp. in light grey) from the Central Range, Taiwan. Analytical uncertainty is smaller than the point size. The linear fit to the soil (dashed line) and plant (black line) data are shown with 95 % confidence bands shaded grey, returning identical gradients, with soil δ^{15}N $= (-8 \pm 3) \times$ Slope $+ (8.0 \pm 1.6)$‰ and plant δ^{15}N $= (-9 \pm 3) \times$ Slope $+ (3.4 \pm 1.3)$‰.

(Table 2). The statistical link between these variables in the soil dataset may be the product of the negative correlation between MAT and slope at the soil sites (Table 1). It can explain why the soil δ^{15}N–MAP and δ^{15}N–MAT trends are opposite to those generally observed elsewhere in tropical forests (Amundson et al., 2003; Craine et al., 2009).

Measured soil δ^{15}N values were higher than plants (Fig. 2), and mean values of these populations were significantly different at the 0.05 level (one-way ANOVA; $P < 0.0001$). The offset between soil and plant organic matter, $\Delta\delta^{15}$N$_{s-p}$, was consistent with an uptake of ^{15}N-depleted N by plants (Delwiche and Steyn, 1970; Handley and Raven, 1992), with the average $\Delta\delta^{15}$N$_{s-p} = 4.1 \pm 0.3$‰ ($n = 6$; Table S2) relatively constant across the range of sampled climatic and geomorphic conditions (MAT 10 °C to 20 °C, MAP 2480 mm and 3200 mm, slope angle 20° to 50°). $\Delta\delta^{15}$N$_{s-p}$ was similar to global-scale predictions from ambient MAP and MAT (Amundson et al., 2003) and also consistent with the 4 ± 2‰ offset between the intercepts of the linear trends between slope and δ^{15}N for soil and plants (Fig. 3). The identical gradients of these trends in the independent datasets further supports the statistical analysis which revealed slope as the primary site attribute linked to δ^{15}N.

5 Discussion

5.1 Constraints on rates of N flux from the ecosystem

The balance between the input of N to an ecosystem and the rate of N loss from soil places a first-order control on the amount of bioavailable N for productivity (Fig. 1). Constraining the fluxes of N and the operation of this mass balance is important for understanding how an ecosystem may respond to ongoing anthropogenic perturbation of the N cycle (Matson et al., 1999; Zaehle et al., 2011). In our samples, the soil C/N decreases with increasing ^{14}C age over centuries to millennia (Table 1). This suggests retention of N relative to C in soils across this mountain forest, consistent with heterotrophic consumption of organic compounds. However, it does not preclude N loss from the soil, and here we seek to model the observed C/N evolution to provide insight to the rates of N loss to the environment.

A multi-component, multi-pool soil model (Trumbore, 1993; Baisden et al., 2002a, b; Manzoni and Porporato, 2009) is not appropriate here, because the soil C/N and ^{14}C measurements were made on homogenised, bulk surface soil, integrating a range of grain sizes and organic-mineral aggregates. In addition, soils in the forested mountains of Taiwan are thin, with the base of the saprolite typically at < 0.8 m below surface (Tsai et al., 2001). As such, transport of organic material to deeper horizons can be considered negligible (cf. Yoo et al., 2006). Therefore, we use a single pool soil model, which describes the evolution of bulk soil N as a mass balance of net inputs and outputs (Fig. 1; Brenner et al., 2001). The soil N content over a constant depth (N_s, t N km^{-2}) evolves at a rate (t N km^{-2} yr^{-1}):

$$\frac{dN_s}{dt} = I_{ex} - k_{ex} \cdot N_s, \tag{1}$$

where I_{ex} (t N km^{-2} yr^{-1}) is the sum of external N inputs to the ecosystem (wet and dry N deposition and N fixation) and k_{ex} is the rate constant of the ensemble of pathways of N loss (inorganic and organic, gaseous, dissolved and particulate) to the environment (yr^{-1}). Here we do not attempt to de-convolve these k_{ex} pathways using C/N alone; instead we use δ^{15}N to examine them in more detail in Sect. 5.2. The model assumes that internal N cycling between soil and vegetation (Fig. 1) operates at a steady state. When considering periods shorter than the time required for soil N to turnover, ~ 50–100 yr (Brenner et al., 2001), this assumption does not hold and the model should be adapted to include internal N cycling (e.g. Menge et al., 2009; Brookshire et al., 2012b) which can show marked inter-annual variability (e.g. Owen et al., 2003). However, for periods longer than this turnover time, the evolution of N_s is principally governed by the external loss rate k_{ex} (Brenner et al., 2001; Menge et al., 2009), and Eq. (1) is adequate.

By analogy, the rate of change in soil organic C content (C_s, t C km^{-2}) through time can also be described by mass balance. Here, the soil input is by supply of plant-fixed carbon:

$$\frac{dC_s}{dt} = j_s \cdot C_p - j_{ex} \cdot C_s, \tag{2}$$

where j_s (yr^{-1}) is the rate constant of organic C supply from plants with a C content C_p (t C km^{-2}) and j_{ex} (yr^{-1}) is the rate constant of C loss from soils, adapted from Baisden et al. (2002a). Again, we consider centennial to millennial timescales ($>$ soil C turnover time) for which a steady state assumption is relevant, where $C_p \approx C_s$ for tropical forest (Dixon et al., 1994). The mass balance can then be simplified to

$$\frac{dC_s}{dt} = -j_{net} \cdot C_s, \tag{3}$$

where the variable j_{net} (yr^{-1}) is the net C loss rate constant.

N_s and C_s are modelled at 50 yr intervals to examine the average rate of N loss from soil integrated over the full dataset. This approach is comparable to considering N export at the catchment-scale, where rivers integrate over large areas > 100 km^2 (Lewis et al., 1999). The starting condition is set by the three "modern" soils (assigned ^{14}C age $= 5 \pm 36$ yr) with an average C/N $= 12$ (Table S3). Changes in ^{14}C abundance are attributed fully to radioactive decay of the bulk soil C pool through time, with a decay constant of 1.2097×10^{-4} yr^{-1} (Godwin, 1962), and the 50-yr resolution of the model means that bomb-^{14}C input is not considered (Levin and Hesshaimer, 2000). The variables I_{ex}, k_{net} and j_{net} are then used to minimise the misfit between modelled and measured soil C/N with age (Fig. 4). Best fit solutions have co-variation of j_{net} and k_{ex} for a given I_{ex}. For $I_{ex} = 0$ t N km^{-2} yr^{-1}, the minimised misfit solutions of the model yield a linear relationship, $k_{ex} = 1.017 \times j_{net} - 0.00033$, with a relative C/N misfit of 19.9 %. For $I_{ex} > 0$ t N km^{-2} yr^{-1}, model solutions exhibit a positive non-linear relationship between j_{net} and k_{ex}.

To explore the range of k_{ex} values permitted by the model best fit to the data, constraints on I_{ex} and j_{net} are required. A global compilation from tropical forests shows that I_{ex} values are commonly 0.2–0.4 t N km^{-2} yr^{-1} away from anthropogenic inputs (Brenner et al., 2001). For j_{net}, we note that the bulk soil samples show a net organic C loss with time. Young soils (^{14}C age < 100 yr) have an average C_{org} of 3.11 ± 1.16 % ($n = 4$), which is significantly higher than older soils (^{14}C age > 1000 yr) with an average $C_{org} = 0.67 \pm 0.07$ % ($n = 5$) and a minimum $C_{org} = 0.41$ % at 4169 yr (Table S3). This strongly suggests that $j_{net} > 0$ yr^{-1}. In fact, assuming that C loss alone is responsible for the observed decrease in C_{org} with age, $j_{net} = 4.8 \times 10^{-5}$ yr^{-1}. This is an upper bound, since it is likely that mineral dilution due to progressive weathering of underlying bedrock also acts to reduce C_s. When $I_{ex} = 0.3$ t N km^{-2} yr^{-1} and
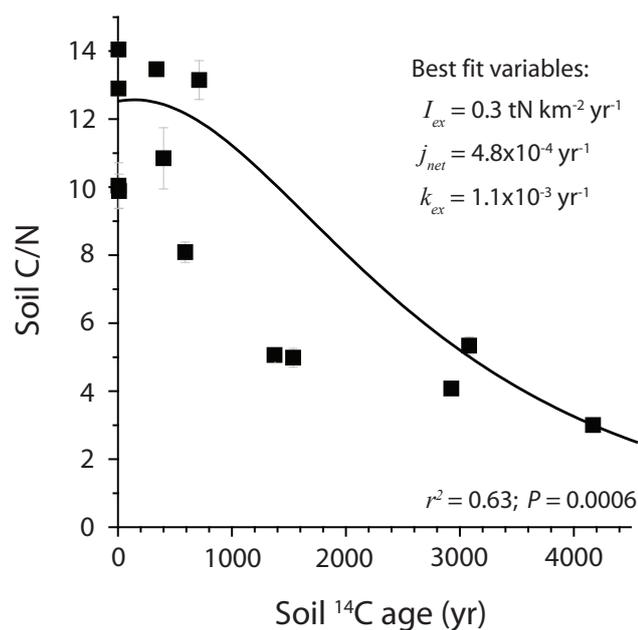
Fig. 4. C/N and ^{14}C age for soil organic matter from the Central Range, Taiwan. Analytical uncertainty is indicated by grey whiskers if larger than the point size. A mass balance model (black line, Eqs. 1 and 3) describes the first-order trend in the data and predicts an integrated average N loss rate constant (k_{ex}) across the dataset, with a minimum misfit parameterisation as shown ($r^2 = 0.63$; $P = 0.0006$).

$j_{net} = 4.8 \times 10^{-5} \, \text{yr}^{-1}$, the fit to the data is strong ($r^2 = 0.63$; $P = 0.0006$), predicting $k_{ex} = 1.1 \times 10^{-3} \, \text{yr}^{-1}$ (Fig. 4). The dependence of k_{ex} on I_{ex} can be explored using the quoted range from tropical forests, returning best fit solutions of $k_{ex} = 0.8 \times 10^{-3} \, \text{yr}^{-1}$ ($I_{ex} = 0.2 \, \text{t N km}^{-2} \, \text{yr}^{-1}$) and $k_{ex} = 1.5 \times 10^{-3} \, \text{yr}^{-1}$ ($I_{ex} = 0.4 \, \text{t N km}^{-2} \, \text{yr}^{-1}$).

The model predictions for the average rate of N loss to the environment, k_{ex}, are consistent with the range of N loss constants in forest ecosystems worldwide (Brenner et al., 2001). However, it is worth remembering that our estimate of k_{ex} is an average for the whole dataset, derived from soils spread over > 100 km (Fig. S1). Deviation from the best fit model (Fig. 4) may reflect local variability in N loss rate around this mean, which is to be expected, but it could also derive from the assumptions applied in the modelling. First, the model misfit was minimised to the measured soil C/N (y-axis), which is justified if the measured ^{14}C ages (x-axis) result only from aging. However, physical erosion can result in thin soils which contain ^{14}C-depleted fossil organic C derived from sedimentary bedrock (Keller and Bacon, 1998). In Taiwan, bedrocks have $C_{org} \sim 0.3\%$ which is incompletely oxidized in the environment (Hilton et al., 2011b). Addition of fossil organic C could increase the ^{14}C age of soil samples, affecting the oldest ^{14}C ages with C_{org} values close to bedrock (Table S3). While mixing of fossil organic C, with C/N ~ 5–10 and no resolvable ^{14}C (Hilton et al., 2010), with

recent biomass is not consistent with the overall trend in the data (Fig. 4), its input could decrease the gradient between C/N and age. This would also occur if any pre-aged POC existed within the soil. Neither of these scenarios are considered by the single pool model (Trumbore, 1993), but they can lead to an underestimation of the rate of change of C/N with time, lowering k_{ex}. Second, the assumption of a steady state exchange between plants and soil (Eqs. 1 and 3) is probably not appropriate for young soils (< 100 yr, $n = 4$), which are prone to progressive N accumulation early in succession (Brenner et al., 2001; Walker and Shiels, 2008). By not accounting for this additional supply, k_{ex} is underestimated by the model at these young sites, but this assumption should not affect the soil C/N versus age relation on longer, multi-centennial timescales (Fig. 4).

Mindful of these caveats, k_{ex} can be converted to an absolute N loss from soils and compared to measured N loss rates. The C stock of soil litter in mixed conifer forests in Taiwan has been measured as $7 \pm 2 \times 10^3 \, \text{t C km}^{-2}$ (Chang et al., 2006), and for the C/N of modern soil organic matter (C/N = 12), the corresponding soil N stock would be $570 \pm 160 \, \text{t N km}^{-2}$. For this stock, the modelled best fit k_{ex} values (0.8–$1.5 \times 10^{-3} \, \text{yr}^{-1}$) are equivalent to an initial N loss rate of 0.5–$0.9 \, \text{t N km yr}^{-1}$ (Fig. 4). This is within the lower range of contemporary estimates of N exports at the river catchment scale, which put leaching of dissolved inorganic N at $0.66 \pm 0.12 \, \text{t N km}^{-2} \, \text{yr}^{-1}$ (Kao et al., 2004) and PN export up to $\sim 1 \, \text{t N km}^{-2} \, \text{yr}^{-1}$ (Sect. 2).

At present, estimated N losses from Taiwanese forests are exceeded by the estimated N deposition of $\sim 1.8 \, \text{t N km}^{-2} \, \text{yr}^{-1}$ from local sources and emissions from continental Asia (Kao et al., 2004). If we consider additional N inputs though symbiotic biological fixation (Vitousek and Howarth, 1991), a contemporary net input of at least $\sim 0.2 \, \text{t N km}^{-2} \, \text{yr}^{-1}$ is supplied to the soil. In contrast, the modelled fit to the ^{14}C and C/N trend suggests that the mountain forest of Taiwan operated with a much closer balance between inputs and outputs prior to the anthropogenic increase in N input (Fig. 4). This finding is consistent with observations from tropical forests elsewhere (Matson et al., 1999) and indicates that N saturation could increasingly affect the Taiwan mountain forest ecosystem if anthropogenic N deposition persists (Aber et al., 1989). Denitrification of a fraction of this accumulated N may produce regionally significant emissions of the greenhouse gas N_2O (e.g. Houlton et al., 2006) and is a poorly understood flux which warrants further assessment in Taiwan (Kao et al., 2004).

5.2 Insight to pathways of N loss from $\delta^{15}N$

The evolution of the soil C/N with ^{14}C age has been used to examine the average rate of N loss permitted by all of the soil data (Fig. 4). While this provides a valuable first-order constraint, individual sites are likely to have N loss rates which vary from this average and experience different pathways of

N loss (e.g. dissolved, gaseous, particulate) depending upon their climatic and geomorphic conditions. While it is difficult to resolve this with C/N, the stable isotope values (δ^{15}N) of soils and plants can provide insight. The δ^{15}N records an integration of N inputs and outputs, and their isotopic signatures (Fig. 1) and δ^{15}N values are sensitive to the modes of N loss and the rates at which they occur (Mariotti et al., 1980; Högberg and Johannisson, 1993; Brenner et al., 2001; Robinson, 2001; Houlton et al., 2006; Hobbie and Högberg, 2012). Hence, we use δ^{15}N values from Taiwan to further interrogate the N cycle operating in this mountain forest.

The decrease in C/N of soil organic matter with soil age is not accompanied by an increase in δ^{15}N values (Table 1). Therefore, the $\sim 6\,‰$ range in δ^{15}N recorded in both soil and plant organic matter is not simply the isotopic expression of accumulated mineral N losses with ecosystem age (cf. Martinelli et al., 1999; Brenner et al., 2001). Instead, the variability in δ^{15}N, which is statistically correlated with slope (Tables 1 and 2), must reflect some combination of (i) variable rates or δ^{15}N of external inputs (Kendall, 1998; Hobbie et al., 1999), and/or (ii) variable rates of fractionating and non-fractionating pathways of N loss (Fig. 1). First, if we consider rates of N input by deposition, it is known that spatial patterns can be complicated in mountainous terrain (Weathers et al., 2006). These authors found that elevation and forest canopy height best explained the spatial pattern of N deposition, with slope angle playing a minor role. In addition, we are not aware of any study in which mycorrhizal fungi distribution and N fixation are linked to hillslope angle (Hobbie et al., 1999; Vitousek et al., 2002). Thus, although we did not measure isotope values of inputs, it is difficult to identify a process by which either the rate of N deposition or its isotopic composition depends systematically on slope, and we still require a mechanistic explanation for the observed in soil and plant δ^{15}N (Fig. 3).

A strong candidate to explain the trends in the data is the loss of PN which operates as a function of slope angle. Hillslope angle is a principal control on the rate of physical erosion (Gilbert, 1909; Culling, 1960; Roering et al., 2001; Dietrich et al., 2003). The stability of hillslope materials is determined by the balance of the down-slope component of its weight and the frictional resistance to motion aided by the slope-normal component of the weight. As the angle increases, this balance shifts in favour of the force driving motion. Therefore, the rate of soil erosion increases with slope ($\sin\theta$) for both overland flow and mass wasting processes such as landsliding (Dietrich et al., 2003; Yoo et al., 2006), and the local topographic gradient should rule the export of PN by soil erosion. Therefore, in analogy to other studies (e.g. Högberg and Johannisson, 1993; Martinelli et al., 1999; Robinson, 2001; Houlton et al., 2006) we seek to explain the variability in δ^{15}N values by gradients in the processes that remove N.

If erosion does not preferentially remove N from plants over soil organic matter, PN loss should impart no direct isotopic fractionation on an ecosystem. However, it can change the bulk isotopic fractionation that the ecosystem experiences due to N loss, and control soil and plant δ^{15}N values (Brenner et al., 2001). To assess whether PN loss can explain the variability in δ^{15}N with slope (Fig. 3), the mass balance model (Eq. 1) can be used to examine δ^{15}N for a given range of k_{ex} values. The solutions at steady state can provide constraint on the sign of the δ^{15}N change and the maximum expected shifts (Brenner et al., 2001). In this case, the ^{15}N/^{14}N ratio of the ecosystem (R_s) is modified from the isotopic ratio of inputs (R_{ex}) by a bulk fractionation factor (α_{ex}) induced by k_{ex}:

$$R_s = \frac{R_{ex}}{\alpha_{ex}}. \tag{4}$$

The rate constant k_{ex} (Eq. 1) includes processes that fractionate isotopes and others that do not (Fig. 1). Fractionating losses can be accounted for by the rate constant k_f (yr^{-1}). These include gaseous loss by denitrification and hydrological leaching of nitrified products, which are generally considered to leave the residual ^{15}N enriched by a fractionation factor $\alpha_f < 1$ (Handley and Raven, 1992). Non-fractioning loss is considered here as PN export (k_E, yr^{-1}) with $\alpha_E = 1$. By definition then, $k_{ex} = k_f + k_E$ (Fig. 1), and so α_{ex} can be determined from the relative contribution of fractionating and non-fractionating losses to total N loss:

$$\alpha_{ex} = \alpha_f \cdot \frac{k_f}{k_{ex}} + \alpha_E \cdot \frac{k_E}{k_{ex}}. \tag{5}$$

Hence, in the absence of any significant change in R_{ex}, R_s (Eq. 4) can vary due to changes in the nature of fractionating losses (α_f), or in the relative importance of non-fractioning pathways to the total N loss (k_E/k_{ex}).

Steady state values for R_s can be calculated using $R_{ex} = 0.0036765$ (atmosphere) and $k_{ex} = 1 \times 10^{-3}$ yr^{-1} derived from the best fit modelled solution of the C/N decrease with ^{14}C age (Fig. 4). The observed range in ecosystem δ^{15}N ($\sim 6\,‰$) is returned for α_{ex} in the range 0.994 to 1.000 (Fig. 5). This can be achieved by varying k_E between 0 yr^{-1} and 1×10^{-3} yr^{-1} while keeping k_{ex} constant and $\alpha_f = 0.994$ (Eq. 5). For these settings and for a soil N stock of $\sim 570 \pm 160$ t N km^{-2}, the PN loss is found to range from zero to 0.6 ± 0.2 t N km^{-2} yr^{-1} across the landscape and averaged over the residence time of N in the ecosystem. This is a lower-bound of the catchment-wide PN erosion rate measured over a few years in the Liwu River and Wulu River catchments, where most of the soil and vegetation samples have been collected (Sect. 2). Due to the expected relationship between k_E and slope for overland flow processes (Dietrich et al., 2003), the mass balance model predicts a linear, negative correlation between δ^{15}N and slope, which is consistent with the soil and plant data from Taiwan (Fig. 3,
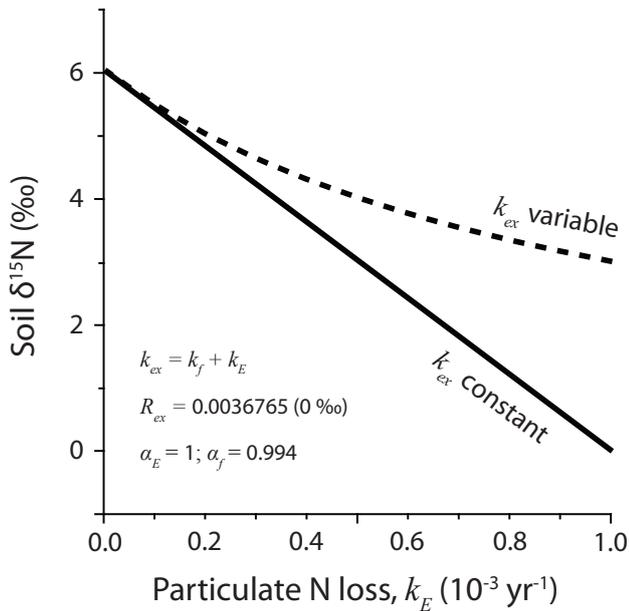
Fig. 5. Mass balance model (Eqs. 1 and 4) predictions of soil δ^{15}N at steady state for a forest experiencing N loss by physical erosion of particulate N, at a loss rate k_E (yr^{-1}). Lines show model scenarios where the total N loss rate k_{ex} (yr^{-1}) remains constant (black line) and increases (dashed line) as k_E increases. The isotopic ratio of inputs (R_{ex}) and the fractionation factor of fractioning losses (α_f) are kept constant with values as shown.

Fig. 6. δ^{15}N and slope for soil and plant organic matter from sites in Peru (squares and triangles) and California (diamonds). Lines and shaded regions show linear fits to the soil and plant samples from Taiwan (Fig. 3). Below $\sin\theta = 0.35$ ($\sim 20°$), erosion rate increases relatively slowly with slope angle. Above this threshold (which relates to thresholds in the activity of erosion processes), soil erosion rates increase rapidly, with a much steeper relationship between slope and erosion rate (Roering et al., 1999). For the Peruvian data, filled symbols are those where $\sin\theta > 0.35$ (see Sect. 5.3).

Tables 1 and 2). Therefore PN loss provides a process-based explanation for the first-order patterns in the data.

We can also use the mass balance model to examine how other N loss processes which fractionate isotopes, k_f (Fig. 1), might vary with slope and impact soil δ^{15}N. The isotopic signatures of fractionating loss processes have not been assessed in Taiwan (Kao et al., 2004; Huang et al., 2012), but the assumed $\alpha_f = 0.994$ is well within the published range of values (Handley and Raven, 1992; Brenner et al., 2001). Gaseous loss can occur under anaerobic conditions in water-logged soils (e.g. Houlton et al., 2006), which are more likely on low slopes. This would imply a decrease in k_f where slopes are steepest. In fact, we model this in the "k_{ex} constant" scenario described above (Fig. 5), where k_f decreases with increasing slope and PN loss becomes relatively more important. However, increased solute leaching on steep slopes could increase k_f, and high rates of dissolved N loss have been observed in mountain forests elsewhere (Brookshire et al., 2012a; Ohte, 2012). To consider these competing controls on k_f, we also model a scenario where k_f remains constant at 1×10^{-3} yr^{-1}, while k_E increases from 0 yr^{-1} to 1×10^{-3} yr^{-1} (i.e. "k_{ex} variable"). This predicts a negative reciprocal relationship between k_E and ecosystem δ^{15}N (Fig. 5). A reciprocal trend between δ^{15}N and slope is also consistent with the soil ($r^2 = 0.35$; $P < 0.0001$) but not the plant data ($r^2 = 0.12$; $P = 0.07$). In this case it is also dif-
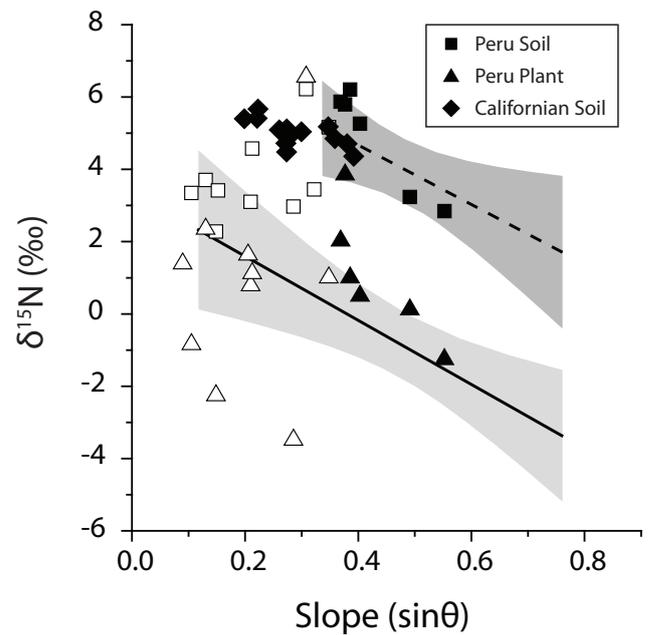
ficult to model the observed variability in δ^{15}N values. The "k_{ex} constant" scenario describes better the first-order pattern in the data (Fig. 3). These findings support the hypothesis of marked heterogeneity in the source of riverine dissolved N from ecosystems (Hedin et al., 2009; Brookshire et al., 2012a) and extend it to PN loss pathways (Fig. 5). It also implies that N loss pathways which fractionate N isotopes may decrease on steep slopes where PN loss dominates export, a geomorphic control on inorganic N pools that warrants further investigation.

5.3 A common geomorphic control on δ^{15}N

The mass balance model demonstrates that the range in plant and soil δ^{15}N in Taiwan can be explained by varying the relative importance of fractionating versus non-fractionating N loss across the mountain landscape (Fig. 5). The negative relationship between soil and plant δ^{15}N values and topographic slope (Fig. 3) is then consistent with an increase in soil erosion and PN loss with increasing slope (Dietrich et al., 2003). While the Taiwan dataset is relatively small (cf. Craine et al., 2009) and it is therefore difficult to make irrefutable conclusions, the new data highlight a plausible mechanism of N loss that has not been widely considered

in the literature (e.g. Brookshire et al., 2012a). Our process-based explanation of the trends in the data should not be unique to Taiwan, but also should affect other mountain forest ecosystems around the world. This hypothesis can be tested more widely with additional field data from different biomes and experimental studies of N loss which are outside the scope of the present study. Herein, we seek existing datasets to evaluate the existence of a possible common geomorphic control on δ^{15}N.

To date, many ecological studies using δ^{15}N have attempted to eliminate slope as an environmental variable when collecting soil and plant samples (e.g. Martinelli et al., 1999; Houlton et al., 2006). In contrast, Townsend-Small et al. (2005) applied a sampling strategy similar to ours, collecting bulk soils and plant organic matter along an elevation transect in the Peruvian Andes. They reported a large range in soil and plant δ^{15}N values, with no significant link between δ^{15}N and temperature (elevation). We reinterpret their data with additional measurements of the local slope at sample sites obtained from the SRTM digital elevation model (90×90 m grid). Further, we also consider published soil data from Marin County, California, where the inverse of slope angle (a proxy for residence time) was used to explain variability in soil δ^{15}N (Amundson et al., 2003).

The Peruvian and Californian soil data are broadly consistent with the findings from Taiwan (Fig. 6). The Californian data exhibit a significant negative correlation between slope and δ^{15}N ($P = 0.007$, $n = 14$) which is stronger than that reported for the inverse of slope (Amundson et al., 2003). On slopes steeper than $\sin\theta = 0.35$, the Peruvian soil data (Townsend-Small et al., 2005) also exhibit a significant negative correlation between slope and δ^{15}N ($P = 0.004$, $n = 7$). Plant samples from multiple species also mirror this trend ($P = 0.05$, $n = 6$). Like Taiwan, both locations experience tectonic convergence, which builds steep topography and promotes high physical erosion rates (Brenner et al., 2001; Townsend-Small et al., 2008). However, on slopes $\sin\theta < 0.35$ the link between soil and plant δ^{15}N values and slope is not significant in the Andean forest (Fig. 6). The switch in behaviour is consistent with the threshold behaviour of geomorphic processes (Roering et al., 1999) and the difference in overall erosion rates between these settings. In headwater catchments of the Andes, physical erosion rates have been estimated at 0.2–0.4 mm yr^{-1} (Safran et al., 2005), 10–20 times lower than those of the Central Range, Taiwan (Dadson et al., 2003). Above $\sim 20°$, the erosion rate increases more rapidly with slope than below this threshold (Roering et al., 1999, 2001). This means that if catchment-wide erosion rates are lower, the reduction in PN loss should be most pronounced on the shallow slopes below this threshold. As a consequence, k_E only becomes significant for the N mass balance on the steepest slopes with the highest erosion rates (when $\sin\theta > 0.35$). On shallower slopes (angle $< 20°$), variability in pathways of fractionating loss (k_f and α_f) or the isotopic expression of N inputs can control δ^{15}N

values as they are thought to do elsewhere (e.g. Hobbie at al., 1999; Houlton et al., 2006). Nevertheless, the commonality between our findings (Fig. 3), the Californian data and steep Andean forest (Fig. 6) suggests that PN removal by physical erosion and its export by mountain rivers can set soil δ^{15}N, and is a major loss term in the N cycle of mountain forests.

PN loss provides a strong coupling between climate and N cycling, which has not previously been recognised (Amundson et al., 2003; Hobbie and Högberg, 2012). It arises because physical erosion rates and erosion of biomass from mountain forest are closely linked to the amount and variability of precipitation and runoff (Dadson et al., 2003; Milliman and Farnsworth, 2011; Hilton et al., 2012). Our findings suggest that a change to a wetter and/or stormier, more erosive climate may impact the N cycle of forests by enhanced PN loss. However, in Taiwan this effect is subsumed at present by significant anthropogenic N inputs, which exceed PN export by physical erosion, explaining the combination of high N export rates and inferred N rich conditions in this ecosystem (Kao et al., 2004). Under natural conditions, PN export may reinforce the coupling of N cycling and climate in mountain forests, providing a broader context and motivation for further studies on the impact of erosion on N cycling at the catchment scale.

Supplementary material related to this article is available online at: http://www.biogeosciences.net/10/1693/2013/bg-10-1693-2013-supplement.pdf.

References

Aber, J. D., Nadelhoffer, K. J., Steudler, P., and Melillo, J. M.: Nitrogen saturation in northern forest ecosystems, BioScience, 39, 378–386, doi:10.2307/1311067, 1989.

Amundson, R., Austin, A. T., Schuur, E. A. G., Yoo, K., Matzek, V., Kendall, C., Uebersax, A., Brenner, D., and Baisden, W. T.: Global patterns of the isotopic composition of soil and plant nitrogen, Global Biogeochem. Cy., 17, 1031, doi:10.1029/2002GB001903, 2003.

Baisden, W. T., Amundson, R., Brenner, D. L., Cook, A. C., Kendall, C., and Harden, J. W.: A multiisotope C and N modeling analysis of soil organic matter turnover and transport as a function of soil depth in a California annual grassland soil chronosequence, Global Biogeochem. Cy., 16, 1135, doi:10.1029/2001GB001823, 2002a.

Baisden, W. T., Amundson, R., Cook, A. C., and Brenner, D. L.: Turnover and storage of C and N in five density fractions from California annual grassland surface soils, Global Biogeochem. Cy., 16, 1117, doi:10.1029/2001GB001822, 2002b.

Brenner, D. L., Amundson, R., Baisden, W. T., Kendall, C., and Harden, J.: Soil N and ^{15}N variation with time in a California annual grassland ecosystem, Geochim. Cosmochim. Ac., 65, 4171–4186, doi:10.1016/S0016-7037(01)00699-8, 2001.

Brodie C. R., Heaton, T. H. E., Leng, M. J., Kendrick, C. P., Casford, J. S. L., and Lloyd, J. M.: Evidence for bias in measured δ^{15}N values of terrestrial and aquatic organic materials due to pre-analysis acid treatment, Rapid Commun. Mass Sp., 25, 1089–1099, doi:10.1002/rcm.4970, 2011.

Brookshire, E. N. J., Hedin, L. O., Newbold, J. D., Sigman, D. M., and Jackson, J. K.: Sustained losses of bioavailable nitrogen from montane tropical forests, Nat. Geosci., 5, 123–126, doi:10.1038/ngeo1372, 2012a.

Brookshire, E. N. J., Gerber, S., Menge, D. N. L., and Hedin, L. O.: Large losses of inorganic nitrogen from tropical rainforests suggest a lack of nitrogen limitation, Ecol. Lett., 15, 9–16, doi:10.1111/j.1461-0248.2011.01701.x, 2012b.

Chang, Y. F., Lin, S. T., and Tsai, C. C.: Estimation of soil organic carbon storage in a Cryptomeria plantation forest of northeastern Taiwan, Taiwan J. Forest. Sci., 21, 383–393, 2006.

Craine, J. M., Elmore, A. E., Aidar, M. P. M., Bustamante, M., Dawson, T. E., Hobbie, E. A., Kahmen, A., Mack, M. C., McLauchlan, K. K., Michelsen, A., Nardoto, G. B., Pardo, L. H., Peñuelas, P., Reich, P. B., Schuur, E. A. G., Stock, W. D., Templer, P. H., Virginia, R. A., Welker, J. M., and Wright, I. J.: Global patterns of foliar nitrogen isotopes and their relationships with climate, mycorrhizal fungi, foliar nutrient concentrations, and nitrogen availability, New Phytol., 183, 980–992, 2009.

Culling, W. E. H.: Analytical theory of erosion, J. Geol., 68, 336–344, 1960.

Dadson, S. J., Hovius, N., Chen, H., Dade, W. B., Hsieh, M. L., Willett, S. D., Hu, J. C., Horng, M. J., Chen, M. C., Stark, C. P., Lague, D., and Lin, J. C.: Links between erosion, runoff variability and seismicity in the Taiwan orogen, Nature, 426, 648–651, doi:10.1038/nature02150, 2003.

Delwiche, C. C. and Steyn, P. L.: Nitrogen isotope fractionation in soils and microbial reactions, Environ. Sci. Technol., 4, 929–935, doi:10.1021/es60046a004, 1970.

Dietrich, W. E., Bellugi, D. G., Sklar, L. S., Stock, J. D., Heimsath, A. M., and Roering, J. J.: Geomorphic transport laws for predicting landscape form and dynamics prediction in geomorphology, in: Prediction in geomorphology, edited by: Wilcock, P. R. and Iverson, R. M., American Geophysical Union, Geoph. Monog. Series, 135, 1–30, doi:10.1029/135GM09, 2003.

Dixon, R. K., Brown, S., Houghton, R. A., Solomon, A. M., Trexler, M. C., and Wisniewski, J.: Carbon pools and flux of global forest ecosystems, Science, 263, 185–190, doi:10.1126/science.263.5144.185, 1994.

Evans, J. R.: Photosynthesis and nitrogen relationships in leaves of C-3 plants, Oecologia, 78, 9–19, doi:10.1007/BF00377192, 1989.

Gilbert, G. K.: The convexity of hilltops, J. Geol., 17, 344–350, 1909.

Godwin, H.: Half-life of Radiocarbon, Nature, 195, p. 984, doi:10.1038/195984a0, 1962.

Handley, L. L. and Raven, J. A.: The use of natural abundance of nitrogen isotopes in plant physiology and ecology, Plant Cell Environ., 15, 965–985, doi:10.1111/j.1365-3040.1992.tb01650.x, 1992.

Hatten, J. A., Goñi, M. A., and Wheatcroft, R. A.: Chemical characteristics of particulate organic matter from a small mountainous river in the Oregon Coast Range, USA, Biogeochem., 107, 43–66, doi:10.1007/s10533-010-9529-z, 2012.

Hedin, L. O., Armesto, J. J., and Johnson, A. H.: Patterns of nutrient loss from unpolluted, old-growth temperate forests – Evaluation of biogeochemical theory, Ecology, 76, 493–509, doi:10.2307/1941208, 1995.

Hedin, L. O., Brookshire, E. N. J., Menge, D. N. L., and Barron, A. R.: The nitrogen paradox in tropical forest ecosystems, Annu. Rev. Ecol. Evol. S., 40, 613–635, 2009.

Hilton, R. G., Galy, A., Hovius, N., Chen, M. C., Horng, M. J., and Chen, H.: Tropical-cyclone-driven erosion of the terrestrial biosphere from mountains, Nat. Geosci., 1, 759–762, doi:10.1038/ngeo333, 2008a.

Hilton, R. G., Galy, A., and Hovius, N.: Riverine particulate organic carbon from an active mountain belt: Importance of landslides, Glob. Biogeochem. Cy., 22, GB1017, doi:10.1029/2006GB002905, 2008b.

Hilton, R. G., Galy, A., Hovius, N., Horng, M. J., and Chen, H.: The isotopic composition of particulate organic carbon in mountain rivers of Taiwan, Geochim. Cosmochim. Ac., 74, 3164–3181, doi:10.1016/j.gca.2010.03.004, 2010.

Hilton, R. G., Meunier, P., Hovius, N., Bellingham, P., and Galy, A.: Landslide impact on organic carbon cycling in a temperate montane forest, Earth Surf. Processes, 36, 1670–1679, doi:10.1002/esp.2191, 2011a.

Hilton, R. G., Galy, A., Hovius, N., Horng, M. J., and Chen, H.: Efficient transport of fossil organic carbon to the ocean by steep mountain rivers: An orogenic carbon sequestration mechanism, Geology, 39, 71–74, doi:10.1130/G31352.1, 2011b.

Hilton, R. G., Galy, A., Hovius, N., Kao, S. J., Horng, M. J., and Chen, H.: Climatic and geomorphic controls on the erosion of terrestrial biomass from subtropical mountain forest, Global Biogeochem. Cy., 26, GB3014, doi:10.1029/2012GB004314, 2012.

Hobbie, E. A. and Högberg, P.: Nitrogen isotopes link mycorrhizal fungi and plants to nitrogen dynamics, New Phytol., 196, 367–382, 2012.

Hobbie, E. A., Macko, S. A., and Shugart, H. H.: Patterns in N dynamics and N isotopes during primary succession in Glacier Bay, Alaska, Chem. Geol., 152, 3–11, doi:10.1016/S0009-2541(98)00092-8, 1999.

Högberg, P. and Johannisson, C.: ^{15}N abundance of forests is correlated with losses of nitrogen, Plant Soil, 157, 147–150, 1993.

Houlton, B. Z., Sigman, D. M., and Hedin, L. O.: Isotopic evidence for large gaseous nitrogen losses from tropical rainforests, P. Natl. Acad. Sci. USA, 103, 8745–8750, doi:10.1073/pnas.0510185103, 2006.

Howarth, R. W., Billen, G., Swaney, D., Townsend, A., Jaworski, N., Lajtha, K., Downing, J. A., Elmgren, R., Caraco, N., Jordan, T., Berendse, F., Freney, J., Kudeyarov, V., Murdoch, P., and Zhu, Z. L.: Regional nitrogen budgets and riverine N & P fluxes for the drainages to the North Atlantic Ocean: Natural and human influences, Biogeochemistry, 35, 75–139, doi:10.1007/BF02179825, 1996.

Huang, J.-C., Lee, T.-Y., Kao, S.-J., Hsu, S.-C., Lin, H.-J., and Peng, T.-R.: Land use effect and hydrological control on nitrate yield in subtropical mountainous watersheds, Hydrol. Earth Syst. Sci., 16, 699–714, doi:10.5194/hess-16-699-2012, 2012.

Kao, S. J. and Liu, K. K.: Stable carbon and nitrogen isotope systematics in a human-disturbed watershed (Lanyang-Hsi) in Taiwan and the estimation of biogenic particulate organic carbon and nitrogen fluxes, Global Biogeochem. Cy., 14, 189–198, 2000.

Kao, S. J., Shiah, F. K., and Owen, J. S.: Export of dissolved inorganic nitrogen in a partially cultivated subtropical mountainous watershed in Taiwan, Water Air Soil Poll., 156, 211–228, 2004.

Keller, C. K. and Bacon, D. H.: Soil respiration and georespiration distinguished by transport analyses of vadose CO_2, $^{13}CO_2$ and $^{14}CO_2$, Global Biogeochem. Cy., 12, 361–372, doi:10.1029/98GB00742, 1998.

Kendall, C.: Chapter 16: Tracing nitrogen sources and cycling in catchments, in: Isotope Tracers in: Catchment Hydrology, edited by: Kendall, C. and McDonnell, J. J., Elsevier Science B.V., Amsterdam, 519–576, 1998.

Körner, C., Farquhar, G. D., and Roksandic, Z.: A global survey of carbon isotope discrimination in plants from high-altitude, Oecologia, 74, 623–632, 1988.

Larsen, M. C., Torres-Sanchez, A. J., and Concepcion, I. M.: Slopewash, surface runoff and fine litter transport in forest and landslide scars in humid tropical steeplands, Luquillo experimental forest, Puerto Rico, Earth Surf. Processes, 24, 481–502, 1999.

Levin, I. and Hesshaimer, V.: Radiocarbon – A unique tracer of global carbon dynamics, Radiocarbon, 42, 69–80, 2000.

Lewis, W. M., Hamilton, S. R. and Saunders, J. F.: Rivers of Northern South America, in: Ecosystems of the World: edited by: Rivers, Cushing, C. and Cummins, K., Elsevier, Dordrecht, Netherlands, 219–256, 1995.

Lewis, W. M., Melack, J., McDowell, W., McClain, M., and Richey, J.: Nitrogen yields from undisturbed watersheds in the Americas, Biogeochem., 46, 149–162, 1999.

Liu, C. P., Yeh, H. W., and Sheu, B. H.: N isotopes and N cycle in a 35-year-old plantation of the Guandaushi subtropical forest ecosystem, central Taiwan, Forest Ecol. Manag., 235, 84–87, doi:10.1016/j.foreco.2006.07.026, 2006.

Manzoni, S. and Porporato, A.: Soil carbon and nitrogen mineralization: Theory and models across scales, Soil Biol. Biochem., 41, 1355–1379, doi:10.1016/j.soilbio.2009.02.031, 2009.

Mariotti, A.: Atmospheric nitrogen is a reliable standard for natural ^{15}N abundance measurements, Nature, 303, 685–687, 1983.

Mariotti, A., Pierre, D., Vedy, J. C., Bruckert, S., and Guillemot, J.: The abundance of natural nitrogen 15 in the organic matter of soils along an altitudinal gradient, Catena, 7, 293–300, 1980.

Martinelli, L. A., Piccolo, M. C., Townsend, A. R., Vitousek, P. M., Cuevas, E., McDowell, W., Robertson, G. P., Santos, O. C., and Treseder, K.: Nitrogen stable isotopic composition of leaves and soil: Tropical versus temperate forests, Biogeochemistry, 46, 45–65, doi:10.1007/BF01007573, 1999.

Matson, P. A., McDowell, W. H., Townsend, A. R., and Vitousek, P. M.: The globalization of N deposition: ecosystem consequences in tropical environments, Biogeochemistry, 46, 67–83, doi:10.1007/BF01007574, 1999.

McClain, M. E. and Naimen, R. J.: Andean Influences on the Biogeochemistry and Ecology of the Amazon River, BioScience, 58, 325–338, 2008.

McGroddy, M. E., Baisden, W. T., and Hedin, L. O.: Stoichiometry of hydrological C, N, and P losses across climate and geology: An environmental matrix approach across New Zealand primary forests, Global Biogeochem. Cy., 22, GB1026, doi:10.1029/2007GB003005, 2008.

Menge, D. N. L., Pacala, S. W., and Hedin, L. O.: Emergence and maintenance of nutrient limitation over multiple timescales in terrestrial ecosystems, Am. Nat., 173, 164–175, doi:10.1086/595749, 2009.

Milliman, J. D. and Farnsworth, K. L.: River Discharge to the Coastal Ocean: A Global Synthesis, Cambridge University Press, Cambridge, UK, doi:10.1017/CBO9780511781247, 2011.

Ohte, N.: Implications of seasonal variation in nitrate export from forested ecosystems: a review from the hydrological perspective of ecosystem dynamics, Ecol. Res., 27, 657–665, doi:10.1007/s11284-012-0956-2, 2012.

Oren, R., Ellsworth, D. S., Johnsen, K. H., Phillips, N., Ewers, B. E., Maier, C., Schäfer, K. V. R., McCarthy, H., Hendrey, G., McNulty, S. G., and Katul, G. G.: Soil fertility limits carbon sequestration by forest ecosystems in a CO_2-enriched atmosphere, Nature, 411, 469–472, doi:10.1038/35078064, 2001.

Owen, J. S., Wang, M. K., Wang, C. H., King, H. B., and Sun, H. L.: Net N mineralization and nitrification rates in a forested ecosystem in northeastern Taiwan, Forest Ecol. Manag., 176, 519–530, 2003.

Quinton, J. N., Govers, G., Van Oost, K., and Bardgett, R. D.: The impact of agricultural soil erosion on biogeochemical cycling, Nat. Geosci., 3, 311–314, doi:10.1038/ngeo838, 2010.

Robinson, D.: Delta N-15 as an integrator of the nitrogen cycle, Trends Ecol. Evol., 16, 153–162, doi:10.1016/S0169-5347(00)02098-X, 2001.

Roering, J. J., Kirchner, J. W., and Dietrich, W. E.: Evidence for nonlinear, diffusive sediment transport on hillslopes and implications for landscape morphology, Water Resour. Res., 35, 853–870, 1999.

Roering, J. J., Kirchner, J. W., and Dietrich, W. E.: Hillslope evolution by nonlinear, slope-dependent transport: Steady-state morphology and equilibrium adjustment timescales, J. Geophys. Res., 106, 16499–16513, doi:10.1029/2001JB000323, 2001.

Safran, E. B., Bierman, P. R., Aalto, R., Dunne, T., Whipple, K. X., and Caffee, M.: Erosion rates driven by channel network incision in the Bolivian Andes, Earth Surf. Processes, 30, 1007–1024, doi:10.1002/esp.1259, 2005.

Saunders, T. J., McClain, M. E., and Llerena, C. A.: The biogeochemistry of dissolved nitrogen, phosphorus, and organic carbon along terrestrial-aquatic flowpaths of a montane headwater catchment in the Peruvian Amazon, Hydrol. Process., 20, 2549–2562, doi:10.1002/hyp.6215, 2006.

Schlesinger, W. H., Reckhow, K. H., and Bernhardt, E. S.: Global change: The nitrogen cycle and rivers, Water Resour. Res., 42, W03S06, doi:10.1029/2005WR004300, 2006.

Shearer, G., Duffy, J., Kohl, K.H., and Commoner, B.: A steady-state model of isotopic fractionation accompanying nitrogen transformations in soil, Soil Sci. Soc. Am. J., 38, 315–322, 1974.

Smith, B. N. and Epstein, S.: 2 categories of ^{13}C/^{12}C ratios for higher plants, Plant Physiol., 47, 380–384, 1971.

Su, H. J.: Studies on the climate and vegetation types of the natural forests in Taiwan: 1. Analysis of the variation in climatic factors, Q. J. Chin. For., 17, 1–14, 1984.

Townsend-Small, A., McClain, M. E., and Brandes, J. A.: Contributions of carbon and nitrogen from the Andes Mountains to the Amazon River: Evidence from an elevational gradient of soils, plants, and river material, Limnol. Oceanogr., 50, 672–685, 2005.

Townsend-Small, A., McClain, M. E., Hall, B., Noguera, J. L., Llerena, C. A., and Brandes, J. A.: Suspended sediments and organic matter in mountain headwaters of the Amazon River: Results from a 1-year time series study in the central Peruvian Andes, Geochim. Cosmochim. Ac., 72, 732–740, doi:10.1016/j.gca.2007.11.020, 2008.

Trumbore, S. E.: Comparison of carbon dynamics in tropical and temperate soils using radiocarbon measurements, Global Biogeochem. Cy., 7, 275–290, 1993.

Tsai, C. C., Chen, Z. S., Duh, C. T., and Horng, F. W.: Prediction of soil depth using a soil-landscape regression model: A case study on forest soils in southern Taiwan, Proc. Natl. Sci. Counc. ROC(B), 26, 34–39, 2001.

Vitousek, P. M. and Howarth, R. W.: Nitrogen limitation on land and in the sea – how can it occur, Biogeochemistry, 13, 87–115, 1991.

Vitousek, P. M., Cassman, K., Cleveland, C., Crews, T., Field, C. B., Grimm, N. B., Howarth, R. W., Marino, R., Martinelli, L., Rastetter, E. B., and Sprent, J. I.: Towards an ecological understanding of biological nitrogen fixation, Biogeochemistry, 57, 1–45, 2002.

Walker, L. W. and Shiels, A. B.: Post-disturbance erosion impacts carbon fluxes and plant succession on recent tropical landslides, Plant Soil, 313, 205–0216, doi:10.1007/s11104-008-9692-3, 2008.

Weathers, K. C., Simkin, S. M., Lovett, G. M., and Lindberg, S. E.: Empirical modeling of atmospheric deposition in mountainous landscapes, Ecol. Appl., 16, 1590–1607, doi:10.1890/1051-0761(2006)016[1590:EMOADI]2.0.CO;2, 2006.

West, A. J., Lin, C. W., Lin, T. C., Hilton, R. G., Liu, S.H., Chang, C. T., Lin, K. C., Galy, A., Sparkes, R. B., and Hovius, N.: Mobilization and transport of coarse woody debris to the oceans triggered by an extreme tropical storm, Limnol. Oceanogr., 56, 77–85, doi:10.4319/lo.2011.56.1.0077, 2011.

Yoo, K., Amundson, R., Heimsath, A., and Dietrich, W. E.: Spatial patterns of soil organic carbon on hillslopes: Integrating geomorphic processes and the biological C cycle, Geoderma, 130, 47–65, 2006.

Zaehle, S., Ciais, P., Friend, A. D., and Prieur, V.: Carbon benefits of anthropogenic reactive nitrogen offset by nitrous oxide emissions, Nat. Geosci., 4, 601–605, doi:10.1038/NGEO1207, 2011.